Available online at www.sciencedirect.com
ScienceDirect
Sedimentary Geology 202 (2007) 821–837
Sedimentary Geology
www.elsevier.com/locate/sedgeo

Distribution, origin and transport process of boulders deposited by the 2004 Indian Ocean tsunami at Pakarang Cape, Thailand

Kazuhisa Goto [a,*], Suchana A. Chavanich [b], Fumihiko Imamura [a], Passkorn Kunthasap [c], Takafumi Matsui [d], Koji Minoura [e], Daisuke Sugawara [e], Hideaki Yanagisawa [a]

[a] *Disaster Control Research Center, Graduate School of Engineering, Tohoku University, Aoba 06-6-11, Aramaki, Sendai 980-8579, Japan*
[b] *Department of Marine Science, Faculty of Science, Chulalongkorn University, Bangkok 10330, Thailand*
[c] *Department of Mineral Resources, Environmental Geology Division, Rama VI Road Ratchtawi, Bangkok 10400, Thailand*
[d] *Department of Complexity Science and Engineering, Graduate School of Frontier Science, The University of Tokyo, 7-3-1 Hongo, Tokyo 113-0033, Japan*
[e] *Institute of Geology and Paleontology, Graduate School of Science, Tohoku University, Aoba, Aramaki, Sendai 980-8578, Japan*

Received 1 December 2006; received in revised form 16 September 2007; accepted 28 September 2007

Abstract

The tsunami of 2004 in the Indian Ocean transported thousands of meters-long boulders shoreward at Pakarang Cape, Thailand. We investigated size, position and long axis orientation of 467 boulders at the cape. Most of boulders found at the cape are well rounded, ellipsoid in shape, without sharp broken edges. They were fragments of reef rocks and their sizes were estimated to be $< 14 m^3$ (22.7t). The distribution pattern and orientation of long axis of boulders reflect the inundation pattern and behavior of the tsunami waves. It was found that there is no clear evidence indicating monotonous fine/coarse shoreward trends of these boulders along each transect line. On the other hand, the large boulders were deposited repeatedly along the three arcuate lines at the intertidal zone with a spacing of approximately 136m interval. This distribution pattern may suggest that long-lasting oscillatory flows might have repositioned the boulders and separated the big ones from small. No boulders were found on land, indicating that the hydraulic force of the tsunami wave rapidly dissipated on reaching the land due to the higher bottom friction and the presence of a steep slope. We further conducted numerical calculation of tsunami inundation at Pakarang Cape. According to the calculation, the sea receded and the major part of the tidal bench (area with boulders at present) was exposed above the sea surface before the arrival of the first tsunami wave. The first tsunami wave arrived at the cape from west to east at approximately 130min after the tsunami generation, and then inundated inlands. Our calculation shows that tsunami wave was focused around the offshore by a small cove at the reef edge and spread afterwards in a fan-like shape on the tidal bench. The critical wave velocities necessary to move the largest and average-size boulders by sliding can be estimated to be approximately 3.2 and 2.0m/s, respectively. The numerical result indicates that the maximum current velocity of the first tsunami wave was estimated to be from 8 to 15m/s between the reef edge and approximately 500m further offshore. This range is large enough for moving even the largest boulder shoreward. These suggest that the tsunami waves that were directed eastward, struck the reef rocks and coral colonies, originally located on the shallow sea bottom near the reef edge, and detached and transported the boulders shoreward.
© 2007 Elsevier B.V. All rights reserved.

Keywords: The 2004 Indian Ocean tsunami; Tsunami boulder; Pakarang Cape; Thailand

* Corresponding author. Tel.: +81 22 795 7515.
E-mail addresses: kgoto@tsunami2.civil.tohoku.ac.jp (K. Goto), csuchana@sc.chula.ac.th (S.A. Chavanich), imamura@tsunami2.civil.tohoku.ac.jp (F. Imamura), passkornk@hotmail.com (P. Kunthasap), matsui@k.u-tokyo.ac.jp (T. Matsui), minoura@mail.tains.tohoku.ac.jp (K. Minoura), sugawara@dges.tohoku.ac.jp (D. Sugawara), yanagi@tsunami2.civil.tohoku.ac.jp (H. Yanagisawa).

0037-0738/$ - see front matter © 2007 Elsevier B.V. All rights reserved.
doi:10.1016/j.sedgeo.2007.09.004

1. Introduction

Large tsunami waves can transport huge boulders as well as sandy sediments. A typical example with historical documents and geologic evidence is the hundreds of scattered reef boulders along the shore of Ishigaki Island, Japan (e.g., Kato and Kimura, 1983; Nakata and Kawana, 1993; Imamura et al., 2001, in press). According to historical documents, these boulders, called "tsunami-*ishi* (stone)" in Japanese, are thought to have been transported as a result of the 1771 Meiwa Yaeyama tsunami, which reached heights of~ 30m (e.g., Kato and Kimura, 1983). Another example is the boulders transported by the tsunami associated with the 1883 Krakatau volcanic eruption (Simkin and Fiske, 1983). Similarly, large boulders having their possible origins in historic or prehistoric tsunamis have been reported worldwide (e. g., Nott, 2000; Mastronuzzi and Sansò, 2000; Noormets et al., 2002; Scheffers et al., 2005; Whelan and Kelletat, 2005; Goff et al., 2006; Morton et al., 2006), though it is still difficult to exclude the possibility of them originating as a result of storms (e. g., Noormets et al., 2002, 2004; Nott, 2004; Morton et al., 2006).

On 26 December 2004, one of the largest tsunamis on record struck the coastal areas around the Indian Ocean (the 2004 Indian Ocean tsunami). On Pakarang Cape, Thailand (Fig. 1a,b), abundant meters-long boulders now scattered along its western shore (Fig. 2b,d,e). No boulders were observed from a satellite image prior to the tsunami even if the tidal level is taken into account (Fig. 2a,c), and these boulders were highly likely transported by the 2004 Indian Ocean tsunami as discussed below. Clarifying the origin of boulders and how these boulders were transported would be important to understand the inundation pattern, the hydrodynamic force, and impact strength to the coast of the tsunami wave currents, because the ability of a tsunami to transport boulders is closely related to the hydraulic force of the tsunami. However, there is no study that investigates the distribution and significance of tsunami boulders just after the tsunami event, and thus it is uncertain what kind of information about tsunami can be obtained from the tsunami boulders. In this context, boulders deposited at Pakarang Cape would provide rare opportunity to study the distribution and significance of tsunami boulders as well as the tsunami inundation pattern and impact to the coastal zone. Thus, we investigated the origin, distribution, and transport process of boulders at Pakarang Cape based on field observation together with numerical calculation.

2. Area description and methods

We conducted field investigations at Pakarang Cape, 13km north of Khao Lak, Thailand (Fig. 1b), from 26 March to 1 April 2005 and from 24 September to 1 October 2005. Although the boulders were also observed in the northern, northeastern, and southern parts of the cape, most of them were found on the western side of the cape (Fig. 2e), where up to 600m offshore the sea floor is a flat and shallow tidal bench composed of reef rocks (Figs. 1c,d, 2a). Thus, we focused our survey to the western side of the cape.

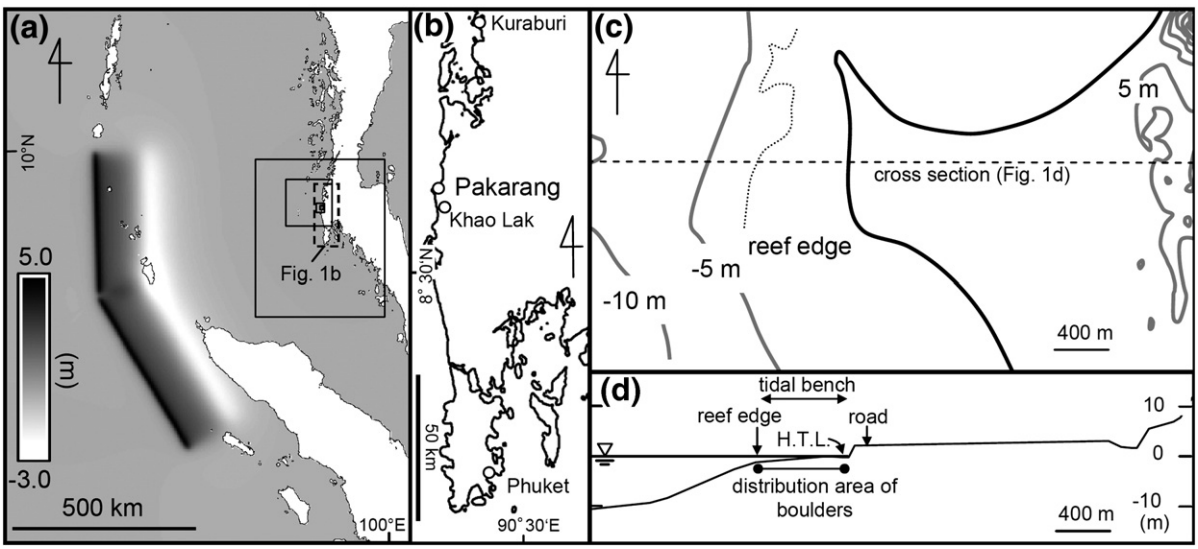

Fig. 1. (a) Location map of the studied area with tsunami source model (based on Takashima et al., 2005). Solid squares show regions for the numerical calculation. (b) Location map of the studied area. (c) Map showing topography/bathymetry around Pakarang Cape. (d) Cross section of the studied area. H.T.L. means high-tide line.

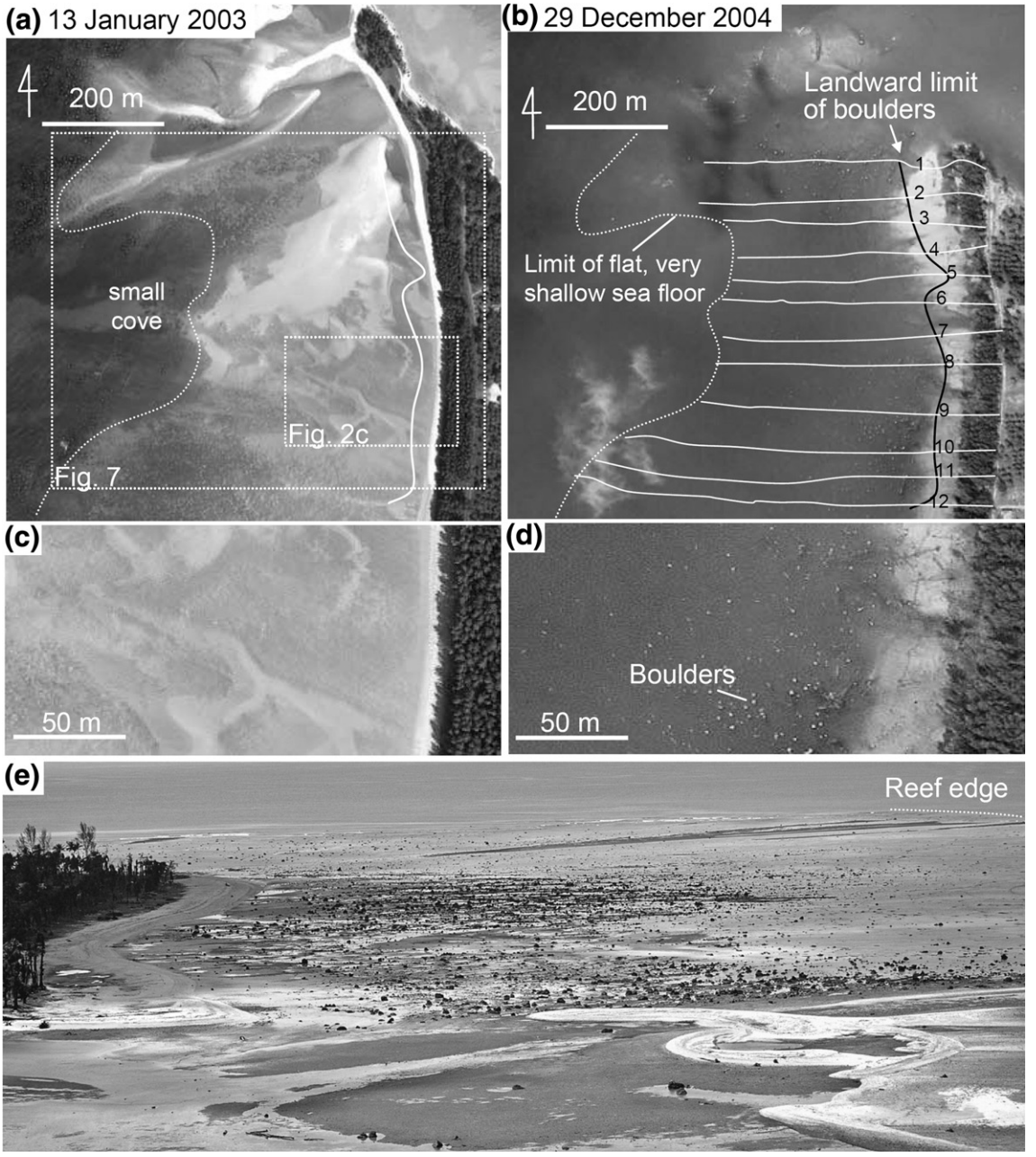

Fig. 2. Satellite images of the western side of the cape (a) before the tsunami (13 January 2003) and (b) after the tsunami (29 December 2004). Note that the shoreline might have been changed after the tsunami due to the sedimentation of sands. The white dashed line in (b) indicates the seaward limit of the flat, very shallow sea floor and is consistent approximately with the likely reef edge. White solid lines indicate transect lines. Close-up satellite images of the cape (c) before and (d) after the tsunami. Boulders are observable after the tsunami, whereas they were absent in the earlier image even if the tidal level is taken into account. These satellite images were provided by Space Imaging/CRISP-Singapore. (e) An oblique south-facing aerial photograph of the cape showing the distribution of the boulders. Note that the landward limit of the boulders is around the high-tide line.

We established twelve shore-normal transects (Fig. 2b; transects 1 to 12 from north to south), approximately 50m apart, extending from a 600-m-long line parallel to the high-tide line to the reef edge. We then measured the dimensions of boulders (totally 467 boulders) along each transect line. We restrict our attention to those boulders having lengths of at least 1m along the long axis. As described below, we identify mainly two different shapes of boulders: circular cone and ellipsoidal in shapes. Since volume is the basis for describing size, we measured the diameter of the bottom

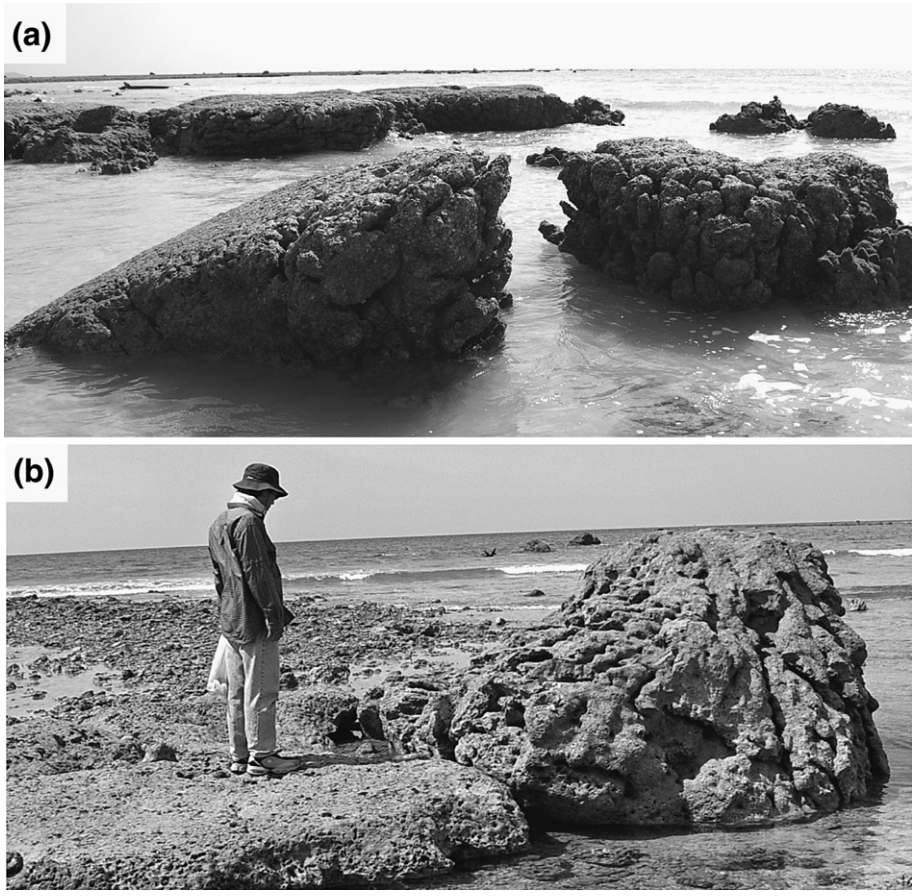

Fig. 3. (a) Reef rocks forming tidal bench around the reef edge. They are largely exposed above the sea level during low tide and were partially broken and tilted. (b) A large boulder showing the typical circular cone in shape with a flat top indicating it is upside down. The boulder is deposited on the tidal bench.

circle and height for boulders that are circular cone in shape. On the other hand, it was difficult to measure the heights for some of the ellipsoidal shaped boulders, because they were partially buried into the sand due to the tidal activity after the tsunami. Thus, we selectively measured the heights of ellipsoidal shaped boulders, which are still clear of the sand. As described below, there is a positive correlation between long axis and height of ellipsoidal shaped boulders. Using this relationship, we estimated the height of partly buried boulders and then calculated corresponding volumes. We also measured the orientations of the long axes of boulders along each line except for those boulders whose long and short axes lengths are similar.

We re-investigated position and orientation of long axes of boulders along transect 1 from 5 to 8 November, 2006 in order to check whether boulders were moved again by the high waves generated by an annual monsoon after our former surveys. Moreover, we conducted underwater surveys by scuba diving technique around Pakarang Cape to investigate the condition of the shallow ocean bottom after the tsunami.

To simulate tsunami propagation in the open sea, we used a linear equation to describe a shallow-water wave on the spherical earth (Goto et al., 1997), with allowance made for the Coriolis force, and to simulate tsunami propagation in the coastal zone and the inundation area, we used a non-linear equation in a Cartesian coordinate system for a shallow-water wave (Goto et al., 1997), with allowance made for bottom friction (Kotani et al., 1998). Governing equations are described as follows:

$$\frac{\partial \eta}{\partial t}+\frac{\partial M}{\partial x}+\frac{\partial N}{\partial y}=0 \tag{2.1}$$

$$\frac{\partial M}{\partial t}+\frac{\partial}{\partial x}\left(\frac{M^2}{D}\right)+\frac{\partial}{\partial y}\left(\frac{MN}{D}\right)+gD\frac{\partial \eta}{\partial x}+\frac{gn^2}{D^{7/3}} \times M\sqrt{M^2+N^2}=0 \tag{2.2}$$

$$\frac{\partial N}{\partial t}+\frac{\partial}{\partial x}\left(\frac{MN}{D}\right)+\frac{\partial}{\partial y}\left(\frac{N^2}{D}\right)+gD\frac{\partial \eta}{\partial y}+\frac{gn^2}{D^{7/3}} \times N\sqrt{M^2+N^2}=0 \tag{2.3}$$

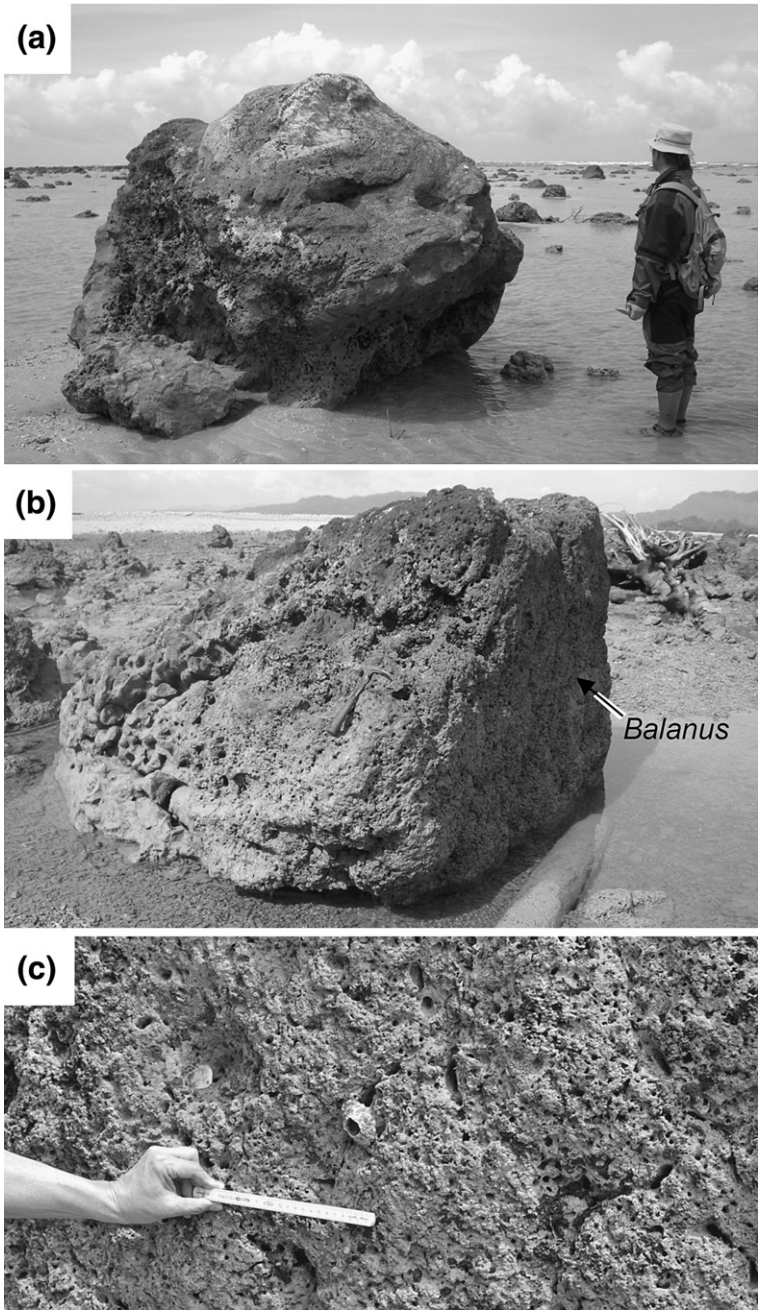

Fig. 4. (a) An typical ellipsoidal shaped boulder and (b) a circular cone shaped boulder. (c) A *Balanus* shell on the flat surface of the boulder in b.

where η is a vertical displacement of water surface above the still water surface, M and N are discharge fluxes in the x- and y-direction, D is a total water depth ($= h + \eta$), and n is a Manning's roughness. The staggered leap-frog method, a finite-difference method, is used to solve equations numerically (Goto et al., 1997), and the condition of the bore front and the Manning's roughness are based on Kotani et al. (1998). We assumed a composite fault model proposed by Takashima et al. (2005) as the source for the tsunami (Fig. 1a). This model reproduces the tidal record measured from satellite (Jason 1) at the Indian Ocean (Takashima et al., 2005), well. The grid-cell size in the region of Pakarang Cape is 17m and calculation time is 300min after the generation of the tsunami (Yanagisawa et al., 2006).

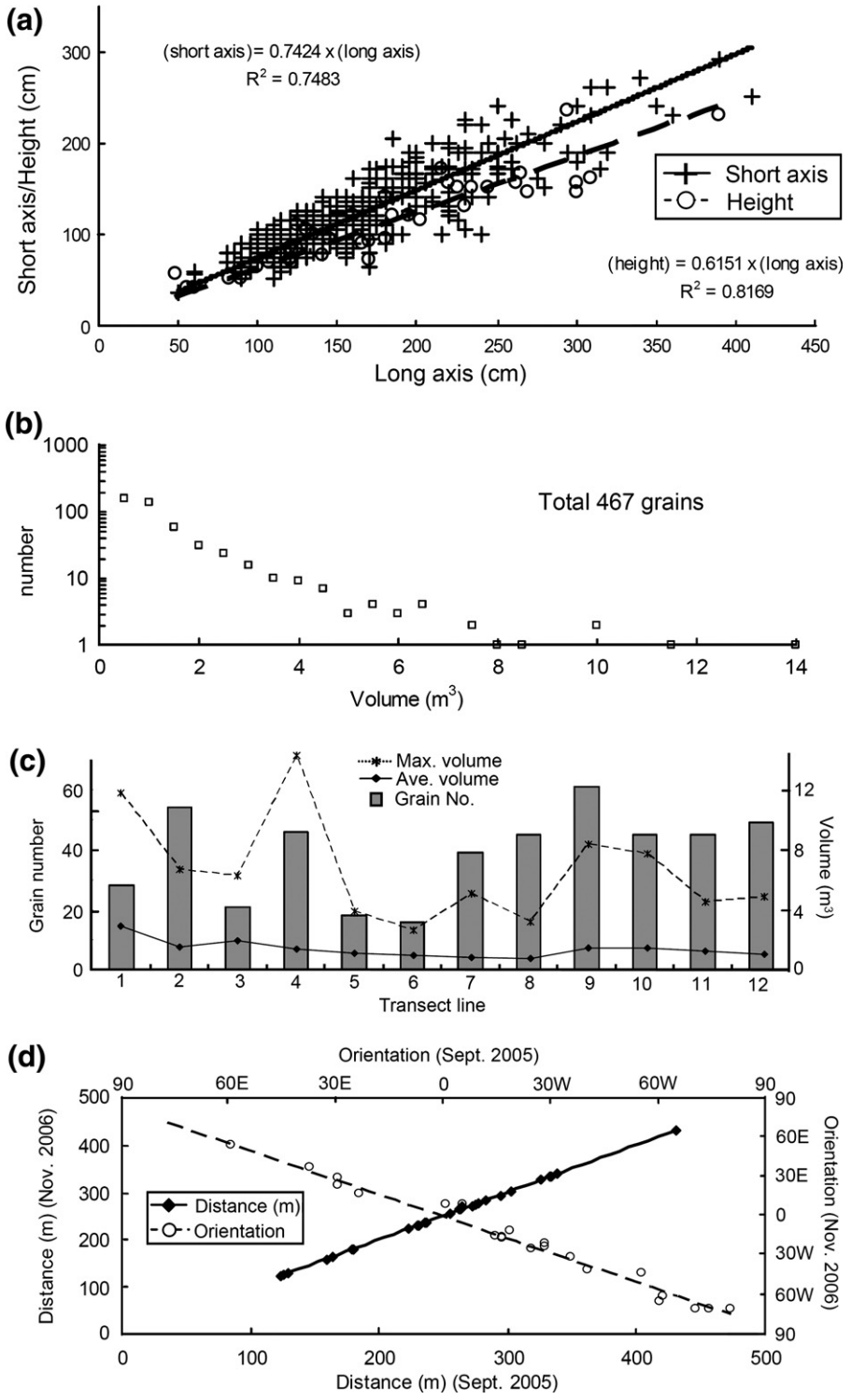

Fig. 5. (a) Diagram showing the relationships between long and short axes, and long axis and height for the case of the ellipsoidal boulders. (b) Diagram showing grain size distribution of boulders. (c) Grain number, maximum volume and average volume of boulders on each transects. (d) Position and long axis directions of boulders along transect 1 on September 2005 and November 2006.

3. Results

3.1. Field observations

More than 1000 boulders are distributed on the western side of the cape, mainly from the high-tide line to the reef edge and over a distance of about 1km from north to south along the shore. No boulders are observed on land above the high-tide line (Fig. 2e). The bottom of the sea from the high-tide line to 200m offshore along each transect is covered by sand- and gravel-sized coral fragments. Between 200m and the reef edge, which lies 300 to 600m offshore, large reef rocks (micro-atolls) form a tidal bench. Some of these micro-atolls were detached and tilted (Fig. 3a). Calcareous algae and some living *Balanus* cover the top surfaces of these rocks. The tidal range at Pakarang Cape is about 4m from the lowest tidal level, and during low tide, the top surfaces of the reef rocks near the reef edge emerge from water (Fig. 3a).

The boulders deposited on the tidal bench (Fig. 3b) are fragments of reef rocks with accreted scleractinian coral colonies consisting of *Porites lutea*, *Galaxea astreata*, *Favia* sp., *Coeloseris mayeri*, *Platygyra daedalea*, and *Leptoria phrygia*. These coral colonies are found at shallow

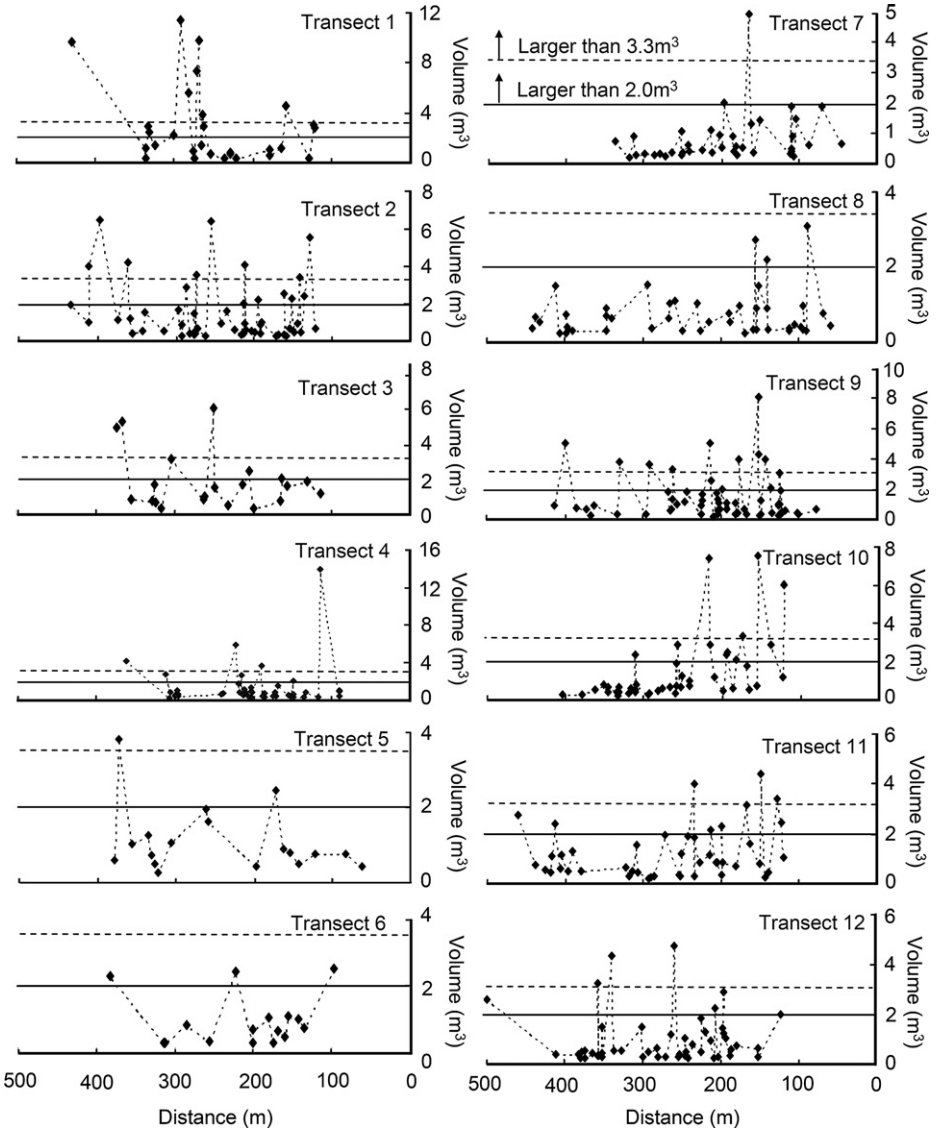

Fig. 6. Grain size distribution of boulders along each transects. Horizontal datum for these plots is indicated in Fig. 7. Black dotted and solid lines divide boulders larger than 3.3 and 2.0 m^3, respectively.

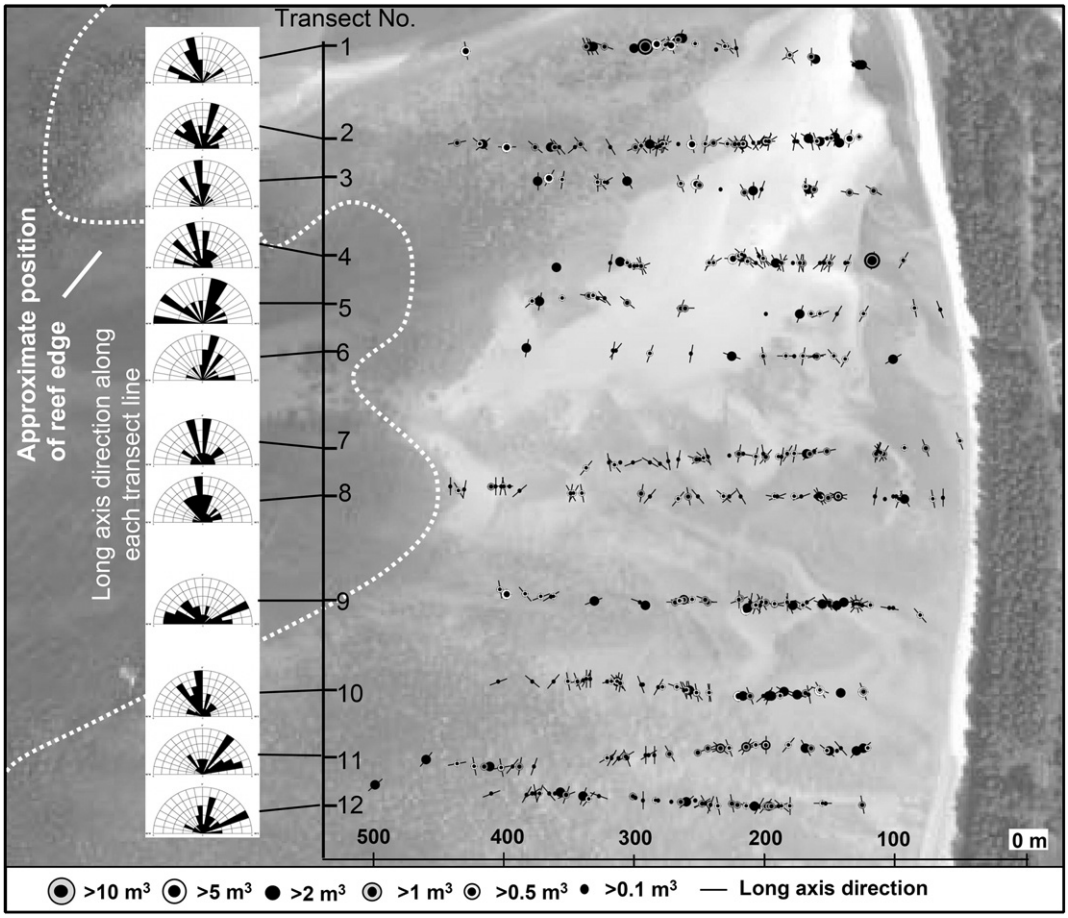

Fig. 7. Map showing the distribution of boulders along each transect line with rose diagrams of the long axes of the boulders. Horizontal axis of rose diagrams indicates the number of boulders, and arc intervals are 10°.

depth, less than 5–10m (e.g., Erhardt and Knop, 2005). Most of corals are not alive now and had probably died before the 2004 Indian Ocean tsunami, since the seawater around the cape, in general, is not conducive for the growth of corals (Dept. Fishery, Thailand, 1999; Benzoni et al., 2006). Boulders are well rounded, ellipsoid to rectangular solid in shape, without sharp broken edges (Fig. 4a). Approximately 4.5% of boulders have circular cone in shape (Fig. 4b) and some of them were apparently upside down (Fig. 3b). Well-preserved tests of barnacles of genus *Balanus* were found to be attached to the flat surfaces of the circular-cone shaped boulders (Fig. 4c), showing its original state and that of the sea level.

The boulders were porous, with densities ranging from 1.46 to 1.7g/cm^3 (1.62g/cm^3 in average). There are positive correlations between long axis and short axis/height of the ellipsoid shaped boulders (Fig. 5a). On the average, the boulders were 1.3m^3 in volume and weigh an estimated 2.1t (Fig. 5b and c). The largest boulder was 14m^3 and had a weight estimated to be about 22.7t. The volumes and numbers of the boulders tend to decrease from transects 1 to 6 and increase from 6 to 12. (Fig. 5c). There was no clear evidence indicating monotonous landward fine/coarse trends of boulders along each transect line (Figs. 6, 7). It is difficult to find systematic distribution pattern of large boulders directly from the Figs. 6 and 7, because small boulders, which were distributed elsewhere in the studied area, hamper to find the distribution trend of large boulders. We will discuss the distribution trend of large boulders in the chapter 4.3. The orientations of the long axes of boulders are variable due to local undulations, but overall they show a dominant NS direction, except for transects 9, 11 and 12 (Fig. 7).

All boulders along transect 1 were at the same position with same orientations of long axes between September 2005 and November 2006 (Fig. 5d). This indicates that high waves generated by the annual monsoon did not have energy enough to move boulders.

According to our underwater surveys, meters-long boulders of reef rocks were also scattered at 4 to 5m water depth, and their concentration decreases toward the deeper zone (~ 10m). Boulders of reef rocks were overgrown by green and red algae and living corals were rarely observed. We identified six coral species (*P. lutea*, *G. astreata*, *Favia* sp., *C. mayeri*, *P. daedalea*, and *L. phrygia*) that were found growing on the boulders at Pakarang Cape. Moreover, coral colonies consisting of *Goniopora* sp., *Acropora formosa*, *Favites abdita*, and *Cyphastrea* sp. were also observed on the surface of reef rocks shallower than 10m water depth. All of these corals are in small sizes approximately 4–5cm in diameter, and this suggests that those live corals recently recruited in the area.

3.2. Numerical calculation

3.2.1. Validity of the numerical results

The tidal gauge closest to Pakarang Cape is Kuraburi (Fig. 1b, Siripong et al., 2005), which is approximately 50km north of the cape. As shown in Fig. 8a, our numerical results reproduce well the wave height and period of the tsunami waves at Kuraburi. The tsunami wave height along the shore at Pakarang Cape was less than 9m (Fig. 8b, Matsutomi et al., 2005; Goto et al., in press). Tsunami wave heights at point A in Fig. 8b are extremely large for comparison with other points. However, the tsunami wave height was measured on trees at point A (Matsutomi et al., 2005), and so might very well be due to

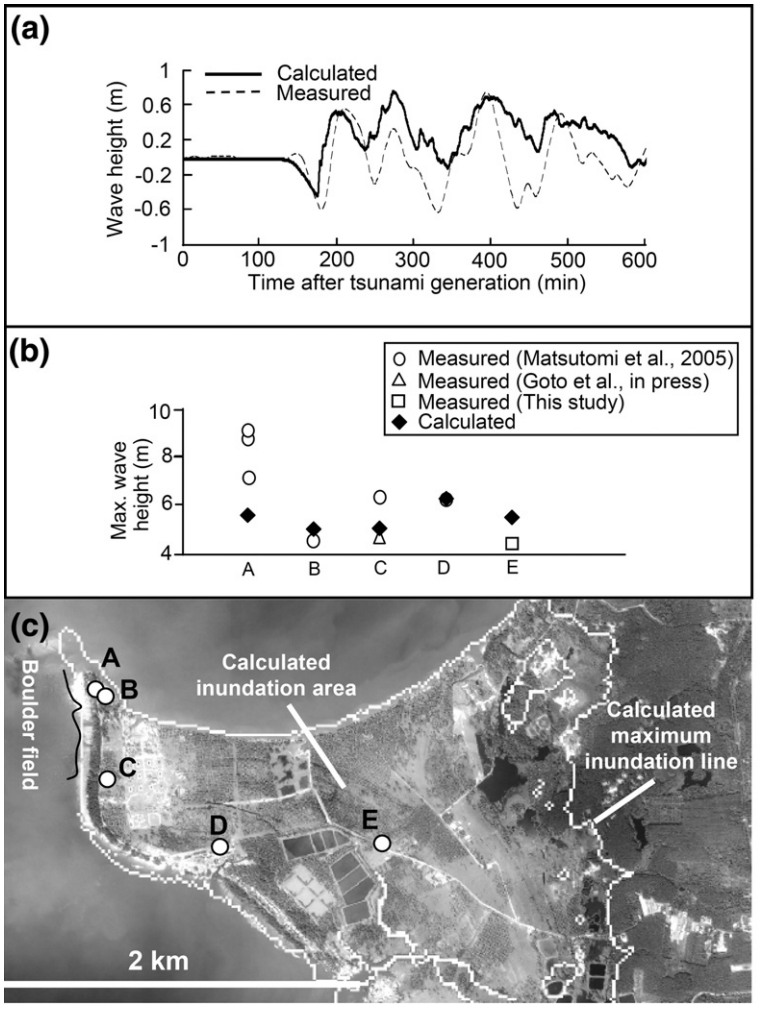

Fig. 8. (a) Diagram showing measured (Siripong et al., 2005) and calculated tidal records at Kuraburi. (b) Diagram showing measured (Matsutomi et al., 2005; Goto et al., in press) and calculated maximum tsunami wave heights at points A to E (see c for the corresponding locations). Tsunami heights were measured on trees at points A and B, and on houses at C, D, and E. Tidal level at the time of the tsunami is the vertical datum for this plot. (c) A satellite image taken after the tsunami around the cape (29 December 2004) with calculated maximum inundation area. The satellite images were provided by Space Imaging/CRISP-Singapore.

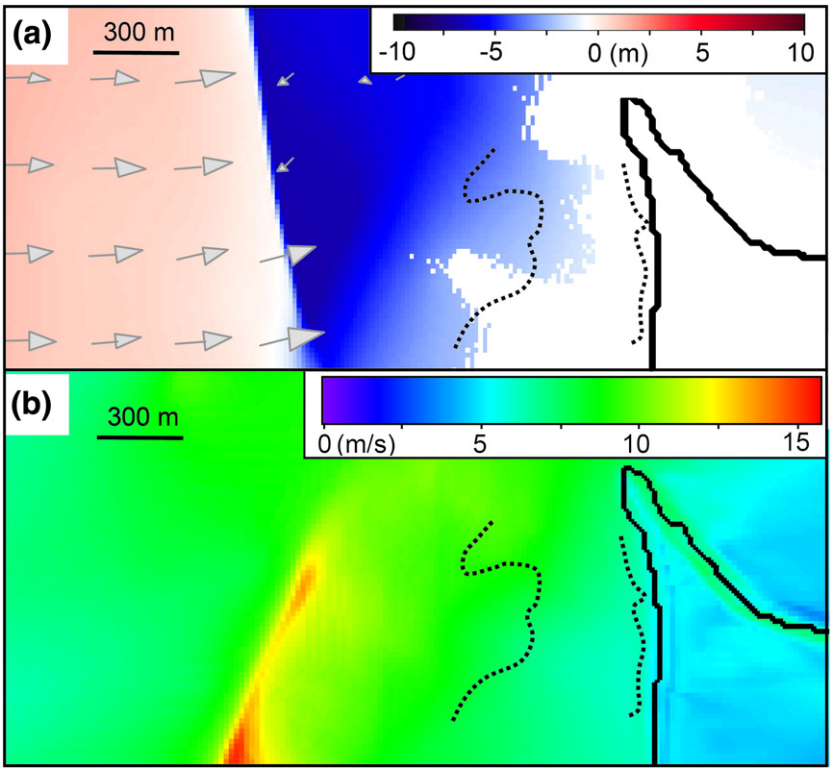

Fig. 9. (a) Numerical result for wave current direction and sea level on the western side of the cape 130 min after the generation of the tsunami, just before the first tsunami wave struck Pakarang Cape. Positive and negative values indicate the sea level above and below the tidal level at the arrival time of the tsunami. Velocities and directions of the tsunami waves are shown by vectors. (b) Numerical result for the maximum tsunami current velocity (m/s) around the cape.

traces of splashes from these waves. On the other hand, wave heights at points C to E were measured on the houses, which could reflect the maximum inundation depth, and thus are more reliable. We interpreted that our numerical results closely model the wave heights around the cape, because calculated maximum wave heights are in good agreement with measured heights at points B to E, although it is underestimated at point A. The inundation area of the tsunami was estimated to be less than 2.5km based on the landward limit of dead grasses as well as from the reports of local residents. The area is also clearly observed in the satellite image after the tsunami (Fig. 8c), and the calculated inundation area agrees well with the observed results (Yanagisawa et al., 2006).

In general, it is difficult to evaluate the validity of the calculated velocity of tsunami currents, because few or no observational data was available for the velocity. Nevertheless, Matsutomi et al. (2006) estimated the current velocity to be 6 to 8m/s at severely damaged buildings along the coast of Khao Lak (Fig. 1b) based on differences in the inundation depth between the front and rear of the structures. Our numerical result gave a value of approximately 6m/s for the maximum current velocity at this site, which is consistent with the estimation by Matsutomi et al. (2006).

In this way, the calculated wave period, inundation area, wave heights, and maximum velocity of the currents around the cape were found to be consistent with the field observations. Thus, we conclude that our numerical results are useful for understanding the transport process of boulders at the cape.

3.2.2. *Calculated inundation process of tsunami at Pakarang Cape*

According to our numerical calculations, the sea receded and the major part of the tidal bench (area with boulders at present) was exposed above the sea surface before the arrival of the first tsunami wave (Fig. 9a). The first tsunami wave arrived at the cape from west to east at approximately 130min after the tsunami generation (Fig. 10a), and then inundated inlands. When tsunami waves reached the reef edge, the wave was focused around the offshore (around transects 5 to 8) by a small cove (Fig. 2a) based on our calculation.

The maximum current velocity of the first tsunami wave was estimated to be from 8 to 15m/s between the

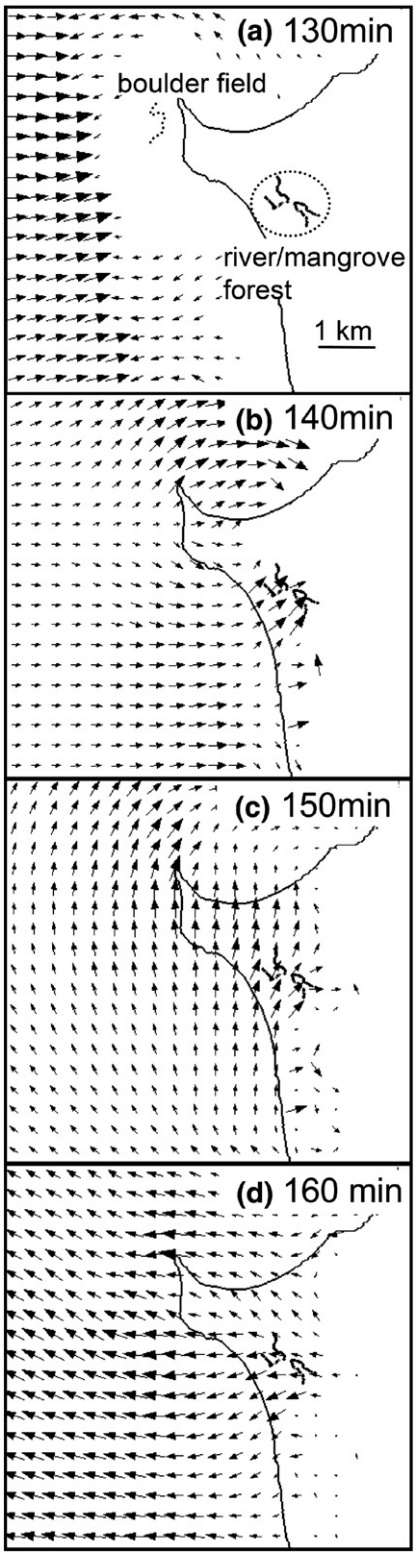

Fig. 10. Snapshots of computing current velocity patterns at (a) 130 (min), (b) 140 (min), (c) 150 (min), and (d) 160 (min) after the generation of the tsunami waves.

reef edge and approximately 500m further offshore, less than 6m/s on the tidal bench, and less than 5m/s on land (Fig. 9b). After the passage of the first tsunami wave front, current velocity decreases over a timespan of 3min and becomes less than 3m/s between the reef edge and approximately 500m further offshore, and less than 2m/s on the tidal bench and on land.

Currents due to the tsunami were concentrated on the cape due to the refraction of the wave (Fig. 10b). The first tsunami wave moving eastward reached only approximately 1km inland from the shoreline at the western part of the cape (Fig. 10b), although inundation area can be estimated to be approximately 2.5km around the studied area. According to our calculation, tsunami waves reached inland deeper along the river at southern part of the cape (Fig. 10b), where mangrove forests were severely damaged (Yanagisawa et al., 2006). The initial inundation along the river covered maximum inundation area (Fig. 10c). This inundation pattern is reasonable, because the river and mangrove forests are topographically lower elevation to the cape and thus the tsunami waves would have concentrated along the river.

Before the arrival of the second wave, northward currents were generated due to the reflection of the wave from south (Fig. 10c). Then, the sea water flows back westward as backwash (Fig. 10d). Current velocity of this backwash at the shoreline is estimated to be less than 3m/s. This velocity is not strong compared to that of the first tsunami wave, because the topography of the area is very flat (Fig. 1c and d). The behavior of subsequent waves becomes complex due to the reflection from surrounding area. Waves of height < 3m continuously arrived at the cape for more than 300min after the generation of the tsunami, and their maximum velocities were estimated to be < 2 to 4.6m/s around the reef edge.

4. Discussion

4.1. Origin of the boulders

Satellite images show no signs of the boulders before the 2004 Indian Ocean tsunami even if the tidal level is taken into account (Fig. 2a and c), whereas they were clearly observed after the tsunami (Fig. 2b and d). The studied site is not in an area affected by strong tropical cyclones (e. g., Neumann, 1993), and, in fact, no strong tropical cyclones occurred between the time the pictures were taken and the tsunami (e.g., Naval Maritime Forecast Center/Joint Typhoon Warning Center, undated). Therefore, tropical cyclones were not responsible for the deposition of the boulders at the cape. These observations, together with the eyewitness reports made by local residents indicate an

absence of boulders before the tsunami, indicate that the boulders were highly likely to have been transported as a result of the 2004 Indian Ocean tsunami.

It can be hypothesized that the boulders had been previously deposited in their present positions and concealed in sands, and that the tsunami eroded the matrix sands, thus exposing the boulders. However, the boulders are distributed on the tidal bench (Fig. 3b), the surface of which corresponds approximately to the mean sea level. This observation suggests that the boulders were not exhumed from sand by the tsunami, but were transported from offshore of the reef edge, and then deposited onto the tidal bench.

Boulders along transect 1 have not changed their position and orientations of long axes between September 2005 and November 2006 (Fig. 5d), although the boulders have experienced a monsoon season between these two surveys. This indicates that high waves generated by the annual monsoon do not have energy enough to move the boulders.

Reef rocks in front of the reef edge and on the shallow sea bottom are similar in shapes and sizes to those of the boulders. Moreover, corals distributed on the boulders of reef rocks in the shallow sea region are the same species as those on boulders deposited on the tidal bench. Reef rocks could have been susceptible to being transported by the tsunami, because they are isolated and not joined together into a reef. In fact, reef rocks around the reef edge were found to be broken and tilted, possibly due to the impact from the tsunami (Fig. 3a). Moreover, Benzoni et al. (2006) observed severe damage and displacement of coral colonies in the offshore shallow sea region at depths lower than 12m in Pakarang Cape (Andaman Sea). Based on these observations, we infer that reef rocks in front of the reef edge and on the shallow sea bottom formed the boulders.

In Thailand, the sea receded before the arrival of the first tsunami wave (Fig. 8a, Siripong et al., 2005). Thus, reef rocks in the shallow sea would have been exposed above the sea level, as is the case during a low tide (Fig. 3a), just before the arrival of the first tsunami wave. This interpretation is supported by the numerical calculations, which shows that the sea receded and the sea level was lowered before the arrival of the first tsunami wave (Fig. 9a). Therefore, reef rocks in front of the reef edge and on the shallow sea bottom could have experienced the strong impact from the first tsunami wave. Thus, we infer that the first, eastward-directed tsunami wave struck and severely damaged the exposed-reef-rocks and coral colonies on the shallow sea bottom offshore of the reef edge.

Most of boulders are well rounded, ellipsoid to rectangular solid in shape, without sharp broken edges. Absence of sharp broken edges probably suggests that these boulders were originally lying on the seabed (scattered or in clusters) in front of the reef edge already before the tsunami. On the other hand, well-preserved tests of barnacles of genus *Balanus* were found to be attached to the flat surfaces of the circular-cone shaped boulders and these boulders could have been originally formed the tidal bench around the reef edge and were broken by the tsunami impact.

4.2. Calculation of critical wave velocity necessary to move the boulder

In this section, we discuss whether the calculated tsunami current velocity exceeds the critical wave velocity necessary to move the boulders. Boulders on the tidal bench at Pakarang Cape are mainly ellipsoidal in shape and they could have moved by rolling rather than sliding, because the friction is lesser for rolling rather than sliding once the boulders are in motion. However, in order to evaluate the movement of boulders under the rigid assumptions, here we assumed boulders as rectangular solid shape and they start to move by sliding.

The critical wave velocity necessary to move the boulder by sliding can be estimated by using the following equations (e. g., Noji et al., 1993). The hydraulic force F acting on the boulder is represented as the sum of the drag and inertia forces (O'Brien and Morison, 1952).

$$F = \frac{1}{2}\rho_f C_D U_f^2 A + C_M \rho_f V \dot{U}_f \quad (1)$$

where ρ_f (= 1.0g/cm^3) is the density of the seawater, C_D (= 2.0) and C_M (= 1.67) are coefficients of drag and mass (e. g., Noji et al., 1993), $\dot{U}_f$ is the current velocity at the position of the boulder, A is the projected area of the boulder against the current, V is the volume of the boulder, and $\dot{U}_f$ is the acceleration of the current. $\dot{U}_f$ is an uncertain parameter, and thus an estimation of the inertia force is usually difficult. However, although the inertia force is effective at the impact of the wave front to the boulders, it decreases suddenly and becomes negligible after the passage of the wave front (e. g., Noji et al., 1993). Because here we adopt the rigid assumption for moving the boulder, we can ignore the inertia force, which acts so as to move the boulder more easily, for simplifying the calculation. The boulders will be displaced when the drag force exceeds the maximum frictional force f at the bottom.

$$F > f (= \mu N) \quad (2)$$

where μ (= 0.75) is the coefficient of static friction, and N is the normal component. With the assumption of a rectangular boulder with its direction of the long axis

perpendicular to that of the current, the critical wave velocities necessary to move the largest and average-size boulders can be estimated to be approximately 3.2 and 2.0m/s, respectively. As stated above, this is a rigid assumption, because inertia force will be effective during the impact of the wave front to the boulders. Moreover, boulders on the tidal bench at Pakarang Cape are mainly ellipsoidal in shape and they could have been moved more easily by rolling than the velocity estimated above.

According to our numerical results, the maximum current velocities of the tsunami between the reef edge and approximately 500m offshore, which is the likely source area for the boulders, were calculated to be 8 to 15m/s (Fig. 9b). This range is large enough for moving the largest boulder shoreward even when we adopt above-mentioned rigid assumptions. These results further support our interpretation that the boulders were transported from offshore near the reef edge. Moreover, the current velocities of subsequent waves at least until 300min after the tsunami generation were estimated to be as low as < 2 to 4.6m/s and are still large enough to move most of the boulders. Therefore, the boulders might have been transported on the tidal bench due to the action of several waves. Moreover, after their deposition on the tidal bench, boulders could have been moved and repositioned by the subsequent wave activities as discussed below.

4.3. Implication for the tsunami inundation pattern from boulder distribution

The orientations of the long axes of boulders are variable, because they are controlled by the local undulations around the area in which they were deposited (Fig. 7). However, the long axes of the boulders generally show a NS direction, except for transects 9, 11, and 12 (Fig. 7). The fact that the boulders are well rounded and ellipsoidal, suggests they were transported by rolling or saltation rather than sliding. Therefore, the long axis orientation should have been perpendicular to the direction of tsunami wave current. The NS trend of long axis orientation of most boulders probably indicates that the direction of the tsunami wave was EW, almost perpendicular to the shoreline. This observation is consistent with our numerical result (Fig. 10).

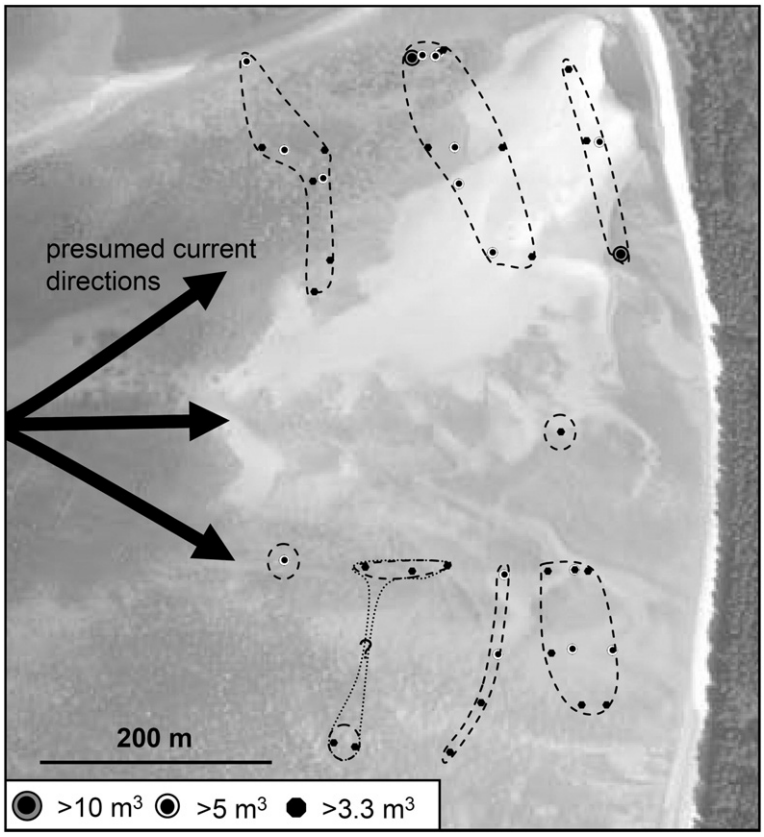

Fig. 11. Map showing distribution area of boulders larger than 3.3 m^3 with presumed current directions.

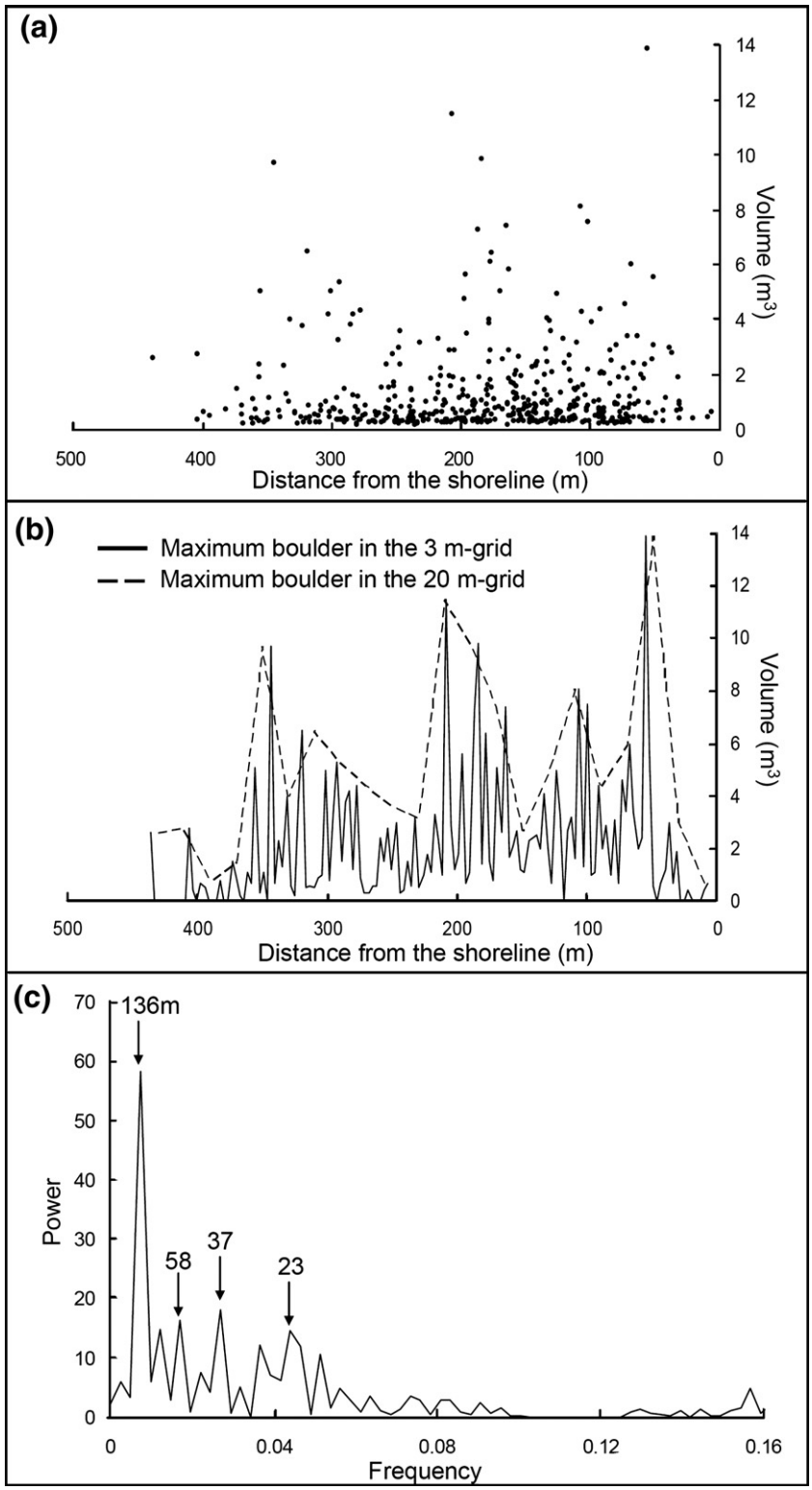

Fig. 12. (a) Grain size distribution of boulders along all transects. Horizontal datum for this plot is the shoreline along each transects. (b) Diagram showing the maximum boulder size in the 3 m-grid cells (solid line) and 20 m-grid cells (dotted line). (c) Result of spectral analysis of boulders (maximum boulders in 3 m-grid cells) by the FFT-method. Three point moving average data was used for this analysis, and linear trend was removed.

There is no clear evidence indicating monotonous fine/coarsening shoreward trends of the boulders along each transect line (Fig. 6). It is difficult to find systematic distribution pattern of large boulders directly from the Figs. 6 and 7, because small boulders, which were distributed elsewhere in the studied area, hamper to find the distribution trend of large boulders. Fig. 11 shows the locations of all boulders larger than 3.3m^3 (43 boulders). As is observed in this figure, these boulders are periodically distributed and are mainly deposited along three arcuate lines along the shoreline.

In order to show the periodicity more quantitatively, we superimposed all transects in one plot (Fig. 12a). This is a strict test, because this plot is expected to be random even if only one transect has a different trend. Instead, there are three peaks, which are formed by the boulders more than 2m^3, separated by an approximately 100–150m interval (Fig. 12a). These peaks do not result from the concentration of large boulders in some specific transects, because large boulders that form these peaks are present in each transect (Fig. 6). We further divided the horizontal axis of this plot into 3m-grid and 20m-grid cells, and traced the maximum boulder size in each grid cell (Fig. 12b). In this figure, several periodic peaks of large boulders are observable. We further conducted spectral analysis using a fast Fourier transformation (FFT) method with the data of maximum boulder size in the 3m-grid cells in order to identify the period of the peaks. As shown in Fig. 12c, there are strong peak at 136m, which corresponds to the interval of the three arcuate lines (Figs. 11, 12a), together with some minor peaks at 58, 37, and 23m.

The arcuate distribution of large boulders probably suggests that the tsunami wave would have inundated from around offshore of transects 5 to 8 and spread afterwards in a fan-like shape on the tidal bench (Fig. 11). This interpretation is plausible because a small cove exists at the reef edge around transects 4 to 9 (Fig. 2a,b), and the tsunami current would have been concentrated in this cove, and then would have spread on the tidal bench.

One possible explanation for the periodic distribution of large boulders with an approximately 136-m-wavelength is that the boulders were transported by three waves. However, boulders might have been transported on the tidal bench by several waves; boulders still have the potential to be repositioned by the long-lasting subsequent waves. Therefore, the effect of subsequent waves should be considered in the interpretation of the distribution of the boulders. In general, the tsunami waves convert to the oscillatory flows along the coast and in the harbor. In fact, megaripples probably reflecting oscillatory flows have been reported on the ground surface in the small forests between the high-tide line and the road at Pakarang Cape (Fig. 1d, Goto et al., in press). When grain sizes are coarse and have a wider range, grain size separation occurs between the crests and troughs of the ripple due to the difference in their mobility (e. g., Friedman et al., 1992). In the same manner, it is possible to speculate that long-lasting oscillatory flows might have occurred between the reef edge and the shoreline, thus moving the boulders repeatedly besides concentrating the bigger ones.

The landward limit of the boulders at Pakarang Cape approximately coincides with the high-tide line; and no boulders were observed on land (Figs. 2e and 7). It can be hypothesized that the boulders had been transported once on land, and were repositioned by the westward backwash afterwards. However, although the velocity of backwash current is slightly higher than the critical velocity necessary to move some small boulders, the boulders probably could not have been moved long distance as a result of this backwash because the current was weak and short in duration due to the very flat topography (Fig. 1d). Therefore, absence of boulders on land probably suggests that the tsunami energy decreased upon reaching the land at the cape. In fact, the calculated current velocity of the tsunami suddenly decreased below the critical velocity necessary to move boulders when the wave reached dry land due to the higher bottom friction and the presence of a steep slope between the high-tide line and the road (Figs. 1d, 9b). The velocity of movement of the boulders would be slower than the velocity of tsunami currents. Hence, the boulders should still be below the high-tide line when the wave front reached land. Therefore, the sudden decreasing of the current velocity upon reaching the land could have resulted in stopping the boulders below the high-tide line.

5. Summary

We conducted a field investigation of boulders deposited by the 2004 Indian Ocean tsunami at Pakarang Cape, Thailand. Thousands of the boulders were found on the western side of the cape, mainly from the high-tide line to the reef edge and over a distance of about 1km from north to south along the shore. No boulders were observed on land above the high-tide line, indicating that the tsunami energy decreased upon reaching the land. The boulders at the cape are fragments of reef rocks and their sizes were found to be < 14m^3. Reef rocks in front of the reef edge and coral

colonies distributed on the shallow sea bottom are the likely source of these boulders. Reef rocks and coral colonies on the shallow sea bottom would have been exposed above the sea level just before the arrival of the first tsunami wave, and they would have experienced the strong impact of the first tsunami wave. There is no clear evidence indicating monotonous landward fining and coarsening of boulders along each transect line, but large boulders tend to concentrate on the three arcuate lines along the shoreline. Arcuate distribution of the larger boulders suggests that the tsunami wave would have caused inundation from around the cove and spread over the tidal bench in a fan shape. Repetitions of small and large boulders were observed at least thrice, indicating long-lasting oscillatory flows which might have repeatedly moved the boulders and separated the large ones from the small ones.

Acknowledgments

We especially thank A. Ruangrassamee, S. Tsukawaki, Y. Fukuda, K. Okada, V. Viyakarn, and U. Darumas for their support during our field survey. The survey was supported by research funds donated to the University of Tokyo (T. Matsui) by T. Yoda, Central Japan Railway Company, Suntory Limited, and WAC Inc. and to Tohoku University by Fukutake Science and Culture Foundation (K. Goto), in part by a Grant-in-Aid from the JSPS (F. Imamura: no. 18201033), and from 21 century COE program of Tohoku University (K. Minoura). We thank three anonymous reviewers and G. J. Weltje for their valuable suggestions and comments.

References

Benzoni, F., Basso, D., Giaccone, T., Pessani, D., Cappelletti, F.S., Leonardi, R., Galli, P., Choowong, M., Di Geronimo, S., Robba, E., 2006. Post-tsunami condition of a coral reef in Leam Pakarang (Andaman Sea, Thailand). Int. Soc. Reef. Studies European Meeting, Bremen, Germany 194.

Department of Fishery, Thailand, 1999. Map of Coral Reefs in Thai Waters: Andaman Sea. Coral Reef Management Project. Department of Fishery Thailand, Bangkok. 198 pp.

Erhardt, H., Knop, D., 2005. Corals: Indo-Pacific Field Guide. IKAN-Unterwasserarchiv, Frankfurt. 303 pp.

Friedman, G.M., Sanders, J.E., Kopaska-Merkel, D.C., 1992. Principles of Sedimentary Deposits. Macmillan Publishing Company, Hampshire. 252 pp.

Goff, J., Dudley, W.C., deMaintenon, M.J., Cain, G., Coney, J.P., 2006. The largest local tsunami in 20th century Hawaii. Mar. Geol. 226, 65–79.

Goto, C., Ogawa, Y., Shuto, N., Imamura, F., 1997. IUGG/IOC Time Project, Numerical method of tsunami simulation with the Leap-Frog scheme. IOC Manuals and Guides. UNESCO, Paris. 130 pp.

Goto, K., Imamura, F., Keerthi, N., Kunthasap, P., Matsui, T., Minoura, K., Ruangrassamee, A., Sugawara, D., Supharatid, S., in press. Distributions and Significances of the 2004 Indian Ocean tsunami deposits — Initial results from Thailand and Sri Lanka-. In: Shiki, T. et al., (Eds.), Tsunamiites — Features and Implications, Elsevier, Berlin.

Imamura, F., Yoshida, I., Moore, A., 2001. Numerical study of the 1771 Meiwa tsunami at Ishigaki Island, Okinawa and the movement of the tsunami stones. Ann. J. Coast. Eng., JSCE 48, 346–350.

Imamura, F., Goto, K., Ohkubo, S., in press. A numerical model for the transport of a boulder by tsunami. J. Geophys. Res. — Ocean. doi:10.1029/2007JC004170.

Kato, Y., Kimura, M., 1983. Age and origin of so-called "*Tsunami-ishi*", Ishigaki Island, Okinawa Prefecture. J. Geol. Soc. Japan 89, 471–474.

Kotani, M., Imamura, F., Shuto, N., 1998. Tsunami run-up simulation and damage estimation by using GIS. Proc. Coast. Eng. JSCE 45, 356–360.

Mastronuzzi, G., Sansò, P., 2000. Boulders transport by catastrophic waves along the Ionian coast of Apulia (southern Italy). Mar. Geol. 170, 93–103.

Matsutomi, H., Takahashi, T., Matsuyama, M., Harada, K., Hiraishi, T., Supartid, S., Nakusakul, S., 2005. The 2004 off Sumatra earthquake tsunami and damage at Khao Lak and Phuket island in Thailand. Ann. J. Coast. Eng., JSCE 52, 1356–1360.

Matsutomi, H., Sakakiyama, T., Nugroho, S., Matsuyama, M., 2006. Aspects of Inundated flow due to the 2004 Indian Ocean tsunami. Coast. Eng. J. 48, 167–195.

Morton, R.A., Richmond, B.M., Jaffe, B.E., Gelfenbaum, G., 2006. reconnaissance investigation of Caribbean extreme wave deposits — preliminary observations, interpretations, and research directions. Open-file report 1293, USGS. 46 pp.

Nakata, T., Kawana, T., 1993. Historical and prehistorical large tsunamis in the southern Ryukyu, Japan. Proceedings, IUGG/IOC International Tsunami Symposium, pp. 297–307.

Neumann, C.J., 1993. Global Overview. In Global Guide to Tropical Cyclone Forecasting, Technical Document WMO/TD 560, Tropical Cyclone Programme Report TCP-31. WMO, Geneva, Switzerland. chapter 1.

Noji, M., Imamura, F., Shuto, N., 1993. Numerical simulation of movement of large rocks transported by tsunamis. Proceedings of IUGG/IOC International Tsunami Symposium, pp. 189–197.

Noormets, R., Felton, E.A., Crook, K.A.W., 2002. Sedimentology of rocky shorelines: 2. Shoreline megaclasts on the north shore of Oahu, Hawaii — origins and history. Sediment. Geol. 150, 31–45.

Noormets, R., Crook, K.A.W., Felton, E.A., 2004. Sedimentology of rocky shorelines: 3: hydrodynamics of megaclast emplacement and transport on a shore platform, Oahu, Hawaii. Sediment. Geol. 172, 41–65.

Nott, J., 2000. Records of prehistoric tsunamis from boulder deposits: evidence from Australia. Sci. Tsunami Hazards 18, 3–14.

Nott, J., 2004. The tsunami hypothesis — comparisons of the field evidence against the effects, on the Western Australian coast, of some of the most powerful storms on Earth. Mar. Geol. 208, 1–12.

O'Brien, M.P., Morison, J.R., 1952. The forces exerted by waves on objects. Trans. Am. Geophys. Union 33, 32–38.

Scheffers, A., Scheffers, S., Kelletat, D., 2005. Paleo-tsunami relics on the southern and central Antillean Island arc. J. Coast. Res. 21, 263–273.

Simkin, T., Fiske, R.S., 1983. Krakatau, 1883: The Volcanic Eruption and Its Effects. Smithsonian Inst. Press, Washington, D. C. 464 pp.

Siripong, A., Choi, B.H., Vichiencharoen, C., Yumuang, S., Sawangphol, N., 2005. The changing coastline on the Andaman seacoasts of Thailand from Indian Ocean tsunami. In: Choi, B.H., Imamura,

F. (Eds.), Proceedings of the Special Asia Tsunami Session at APAC 2005. Hanrimwon Publishing Co., Ltd., Seoul, pp. 21–31.

Takashima, M., Koshimura, S., Meguro, K., 2005. Development of possible tsunami exposure estimation module for tsunami disaster response. Proceedings of the Fourth International Symposium on New Technologies for Urban Safety of Mega Cities in Asia. ISBN: 981-05-4063-9, pp. 481–488.

Whelan, F., Kelletat, D., 2005. Boulder deposits on the southern Spanish Atlantic coast: possible evidence for the 1755 AD Lisbon tsunami? Sci. Tsunami Hazards 23, 25–38.

Yanagisawa, H., Koshimura, S., Goto, K., Imamura, F., Miyagi, T., Hayashi, K., 2006. Tsunami inundation flow in the mangrove forest and criteria of tree damages. — field survey of the 2004 Indian Ocean Tsunami in Khao Lak, Thailand-. Ann. J. Coast. Eng., JSCE 53, 231–235.